IEEE Journal of Translational Engineering in Health and Medicine

Received 10 June 2022; revised 16 November 2022; accepted 16 December 2022.
Date of publication 19 December 2022; date of current version 6 July 2023.

Digital Object Identifier 10.1109/JTEHM.2022.3230716

Automated System for Multiplexing Detection of COVID-19 and Other Respiratory Pathogens

PARKER Y. L. TSANG[1,2], SUNNY L.H. CHU[1,2], LIBBY C. W. LI[1], DEBORAH M. S. TAI[1], BERRY K. C. CHEUNG[1], FIRAOL TAMIRU KEBEDE[2], PETE Y. M. LEUNG[2], WINSTON WONG[1], TERESA CHUNG[2], CYRIL C. Y. YIP[3], ROSANA W. S. POON[3], JONATHAN H. K. CHEN[3], KWOK-YUNG YUEN[3,4], MANSON FOK[1,5], JOHNSON Y. N. LAU[1,6], AND LOK-TING LAU[1,2,7]

[1]Emerging Viral Diagnostics (HK) Ltd., Hong Kong
[2]Department of Industrial and Systems Engineering, The Hong Kong Polytechnic University, Hong Kong
[3]Department of Microbiology, The University of Hong Kong, Hong Kong
[4]Centre for Virology, Vaccinology and Therapeutics, Hong Kong Science and Technology Park, Hong Kong
[5]Faculty of Medicine, Macau University of Science and Technology, Macau
[6]Department of Biology, Hong Kong Baptist University, Hong Kong
[7]School of Chinese Medicine, Hong Kong Baptist University, Hong Kong

CORRESPONDING AUTHOR: LOK-TING LAU (terencelau@hkbu.edu.hk)

This work was supported in part by the Innovation and Technology Fund (ITF) of the Hong Kong, Special Administrative Region of China (HKSAR) Government, in part by the Public Sector Trial Scheme (PSTS) under Grant SST/031/20GP, in part by the Midstream Research Programme for Universities (MRP) under Grant MRP/040/20x, and in part by Health@InnoHK.

This work involved human subjects or animals in its research. Approval of all ethical and experimental procedures and protocols was granted by The Hong Kong Polytechnic University, Human Subjects Ethics Sub-committee, under Protocol No. HSEARS20200806001 on 26 August 2020, and HKU HA HKW IRB under Protocol No. UW 20-224 on 20 March 2020.

This article has supplementary downloadable material available at https://doi.org/10.1109/JTEHM.2022.3230716, provided by the authors.

ABSTRACT *Objective:* Infectious diseases are global health challenge, impacted the communities worldwide particularly in the midst of COVID-19 pandemic. The need of rapid and accurate automated systems for detecting pathogens of concern has always been critical. Ideally, such systems shall detect a large panel of pathogens simultaneously regardless of well-equipped facilities and highly trained operators, thus realizing on-site diagnosis for frontline healthcare providers and in critical locations such as borders and airports. *Methods & Results:* Avalon Automated Multiplex System, AAMST, is developed to automate a series of biochemistry protocols to detect nucleic acid sequences from multiple pathogens in one test. Automated processes include isolation of nucleic acids from unprocessed samples, reverse transcription and two rounds of amplifications. All procedures are carried out in a microfluidic cartridge performed by a desktop analyzer. The system was validated with reference controls and showed good agreement with their laboratory counterparts. In total 63 clinical samples, 13 positives including those from COVID-19 patients and 50 negative cases were detected, consistent with clinical diagnosis using conventional laboratory methods. *Conclusions:* The proposed system has demonstrated promising utility. It would benefit the screening and diagnosis of COVID-19 and other infectious diseases in a simple, rapid and accurate fashion.

INDEX TERMS Automation, biochemistry, COVID-19, clinical diagnosis, genomics, microfluidics, polymerase chain reaction (PCR).

Clinical and Translational Impact Statement— A rapid and multiplex diagnostic system proposed in this work can clinically help to control spread of COVID-19 and other infectious agents as it can provide timely diagnosis, isolation and treatment to patients. Using the system at remoted clinical sites can facilitate early clinical management and surveillance.

I. INTRODUCTION

Infectious diseases pose threats to human health and global stability [1], as witnessed by the ongoing Coronavirus Disease 2019 (COVID-19) pandemics [2] caused by severe acute respiratory syndrome coronavirus 2 (SARS-CoV-2). COVID-19 has spread over all the continents within a few months, leading to millions of deaths, public health crisis and economic plunges in various countries [3]. A rapid and

IEEE Journal of Translational Engineering in Health and Medicine

accurate pathogen detection test that is simple to perform has been impactful for COVID-19 [4]. It can provide informative result for prompt clinical management of infected individuals [4]. It also enables effective surveillance and assists policy makers in devising mitigation approach to prevent pandemics [5], [6].

Cell culture is the conventional approach for pathogen diagnosis [7]. However, the method is laborious with long turnaround time. Since cell culture cannot pick up novel and unculturable species, it is not a universal strategy for pathogen screening [8], [9]. Molecular techniques are now seeing wide applications in clinical diagnosis. Sequencing and microarray are powerful diagnostic and discovery tools that provide comprehensive genetic profiling of infected pathogens. However, large implementation remains challenging owing to high cost and the demand of highly-skilled molecular technologists. Detection based on nucleic acid amplification such as polymerase chain reaction (PCR) and loop-mediated isothermal amplification (LAMP) offers fast turnaround time, particularly when testing volume is high [10]. PCR-based methods offer high diagnostic sensitivity in patients with early symptoms and in asymptomatic subjects [11]. Reverse-transcription PCR (RT-PCR), for example, has been widely adopted for SARS-CoV-2 frontline screening [3], [12] and is considered as gold standard for population-scale testing in COVID-19 pandemic [3]. Another common approach detects pathogen-derived antigens/proteins on a strip. The test can be performed by individuals themselves at low cost. However, it falls short in achieving accuracy and multiplexing potential in comparison to nucleic acid based detection [13], [14].

A major advantage of PCR is that pathogen detection assays can readily be developed with primers designed upon the identified pathogen genomes [15], [16]. ''Nested'' PCR can further improve sensitivity and specificity of the detection, particularly in case of early infection where pathogen-derived nucleic acids present at low abundance in clinical samples [11], [17], [18], [19]. Distinct from conventional PCR, nested PCR involves two sequential amplifications in which the product of the first-stage PCR is used as template for the second-stage PCR [17]. A nested PCR assay involves two primer pairs. The outer-primers are designed for amplifying a larger outer amplicon in first-stage PCR. The inner-primers bind to the amplicon in second-stage PCR. The use of inner-primers can effectively minimize amplification of spurious products, which could be generated by non-specific interaction among primers themselves or with non-target sequences [17], [20].

Multiplex PCR refers to the detection of multiple pathogens or gene targets simultaneously in a single run. Many upper respiratory tract pathogens, including SARS-CoV-2, manifest overlapping clinical symptoms but distinct clinical management. Multiplex PCR is advantageous in differentiating disease-causing pathogens or revealing etiologies that are clinically undefined [21]. Multiplex PCR can also be used for pathogen subtyping, such as to discriminate the strains of H7N9 and H5N1 which are more severe and contiguous than other influenza A strains. Patients co-infected with multiple pathogens can also be readily identified. Hence, multiplex PCR can provide informative diagnostic result. Thus, infected patients can receive appropriate treatment.

Multiplex PCR is conventionally limited to a few detection targets. One major challenge is the complex interference among a large number of primers in the reaction matrix. Careful primer design and thorough experimental evaluation are therefore important. Moreover, multiplex real-time quantitative PCR (qPCR) can be designed with different fluorescent dyes assigned for individual detection targets. However, the number of fluorescent dyes, and hence the number of multiplexing targets is typically limited to <8 due to the overlapping optical spectra of fluorophores [22]. Alternatively, multiple singleplex PCRs, each for different target, can be parallelly run on separated wells of standard multi-well plates. The reaction setup, however, involves tedious pipetting work or relies on expensive liquid handling system. The required volumes of sample and reagents are also increased, posing the considerations of sample availability, infectious risk and reagent cost.

Public accessibility of the PCR-based pathogen tests is still hampered by the requirement of central molecular laboratories. Their setup and operation are expensive and challenging, including a list of well-equipped instruments for contagious handling and trained operators [8]. Qualified infrastructure, equipment, personnel, safety and contamination control shall all assured. Poor management can lead to contamination of pathogens and PCR amplicons, which would interfere testing accuracy and increase the risk of pathogen spreading within the laboratory and even to the outside [10]. Such high barriers to entry also make the tests neither accessible nor affordable to population in remote locations or developing regions. Turnaround time for testing result would be in days due to travelling of samples to central laboratories [23]. Therefore, a point-of-care testing (POCT) system [24] would be a future solution in fighting infectious diseases. In this study, Avalon Automated Multiplex System (AAMST) is developed. It is a 'sample-in-result-out' system with high multiplexing potential based on molecular techniques. In this report, introduction of the underlying biochemistry and the design of AAMST are presented. System is validated using reference control materials and clinical samples. Discussion includes potential significance of the system is given as well.

II. BIOCHEMISTRY WORKFLOW

The underlying testing protocol of the proposed system is based on nested RT-qPCR (Table 1). The workflow starts with adding a sample such as reference control and clinical specimen into a collection tube containing viral transport medium (VTM) which preserves pathogen integrity during transfer of samples to the point of analysis. Nucleic-acid extraction is then followed. Its protocol was optimized to fulfill (i) generalization to most kinds of pathogens including viruses, gram-positive and -negative bacteria and fungi, (ii) comparable extraction efficiencies among various types of clinical specimens that are commonly encountered, and (iii) simultaneous isolation of both deoxyribonucleic acid (DNA) and ribonucleic acid (RNA). Hence, a stringent lysis protocol combining bead-beating and sonication is employed. Lysis

TABLE 1. Workflow of nested RT-qPCR in the AAMST testing protocol.

Step	Step name	Procedures
1	Sample lysis	Sonication and chemical lysis
2	Nucleic acid extraction	Lysate flow through silica membrane
3	RT-PCR[1] (first-stage amplification)	Multiplex RT-PCR[1] (with multiple outer-primer pairs)
4	Dilution of RT-PCR product	67-fold dilution with nuclease-free water
5	qPCR[2] (second-stage amplification and detection)	Singleplex qPCR[2] of individual targets in multiple wells (with a inner-primer pair and a probe for each target assay)

[1]reverse-transcription polymerase-chain-reaction
[2]qPCR, real-time quantitative PCR

buffer is added to the sample for dissociating cell and nuclear membranes, and releasing intact nucleic acids inside. The thick cell walls enclosing bacterial and fungal pathogens, that are resistant to generic lysis buffer, are mechanically disrupted using bead-beating treatment [25]. The product of cell lysis (lysate) is mixed with binding buffer which contains chaotropic salt. Using a centrifuge, the lysate is then passed through a silica membrane, and nucleic acids are isolated by adsorption onto the membrane. The membrane is washed to remove protein and other contaminant. Nucleic acids are finally eluted from the membrane using low-salt buffer.

For nucleic acid amplification, RT and first-stage PCR are performed in a single tube with reaction mixture comprising reverse transcriptase, DNA polymerase, and outer-primer pairs targeting each of the pathogens of interest. It is a *multiplex* reaction in which all targeted RNA sequences are converted to complementary DNA (cDNA) with gene-specific primers in one tube, followed by simultaneous amplification of all targeted DNA and cDNA sequences in the same tube. To increase amplification specificity, the outer-primers are designed to have a high melting temperature of around 65°C. First-stage amplification is carried out for 20 PCR cycles. One advantage of involving first-stage PCR is to increase the amount of template sequences for subsequent qPCR. The detection sensitivity can therefore be improved.

Prior to second-stage qPCR, the amplicons produced from first-stage PCR is diluted approximately 67-fold in order to diminish any inhibition due to residual reagents, primers and contaminants [16], [17], [20]. The diluted amplicons are distributed into tubes for performing *singleplex* qPCRs. For each pathogen target, a pair of inner-primers that anneal to gene sequences downstream the outer-primer binding sites are designed. Second-stage qPCR amplifies the diluted products from first-stage PCR. A TaqMan probe for fluorescent detection is also included for each qPCR assay. The use of inner-primers and TaqMan probe can enhance detection specificity since any non-specifically amplified sequences from first-stage PCR could not be bound and amplified in second-stage qPCR. In laboratory, a thermal cycler is used to perform the qPCR. Fig. 1 elaborates the process with schematic of nucleic acids under this amplification approach.

Amplification efficiencies of all primers and probes were optimized on benchtop, using conventional instruments

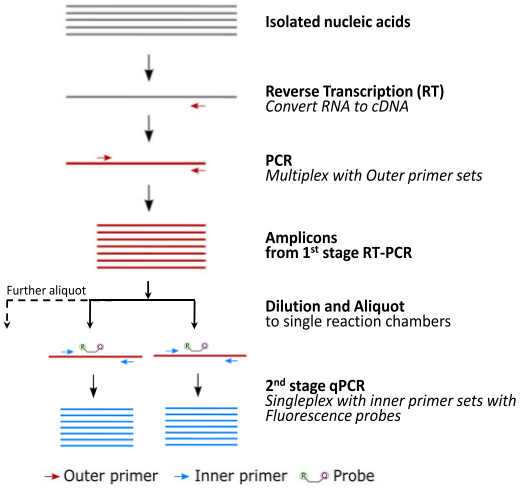

FIGURE 1. Schematic illustration of the biochemistry of RT-qPCR.

and procedures in routine laboratory setting. Primers and probes were designed upon sequence information from National Center for Biotechnology Information (NCBI, https://www.ncbi.nlm.nih.gov/), using either stand-alone open-source software Primer3 (https://primer3.ut.ee/) or were manually designed based on information provided by the Department of Microbiology, University of Hong Kong. The outer and inner primers generated amplicon sizes in ranges of 135 – 334 bp and 72 – 202 bp, respectively. Specificities of the multiplex nested RT-qPCR were confirmed to be equivalent to their singleplex counterparts at equimolar concentrations for all of the pathogens covered in the assay. It is worth noting that such the primer optimization at high-level multiplexing is always challenging. For example, for the 23-plex RT-qPCR developed in this study (Table 2), the presence of 46 outer-primers together in the RT-PCR matrix would lead to a high chance of cross hybridization among the primers and mis-priming of primers to other target sequences. This would affect the proper binding of primers to their designated targets, resulting in poor amplification efficiency and detection sensitivity. Mis-priming would also give rise to cross-reactivity among pathogen targets, leading to false positive result. In our system, these complications can potentially be overcome by the use of nested-PCR and probe-based detection [17], [26]. Also, continual evolving genomes of the pathogens, particularly viruses, may also affect priming and amplification of the assay. One example is influenza A (Flu A) (matrix) RT-qPCR assay (Table 2). During our on-going pre-clinical trial, we observed that the performance of the assay had become sub-optimal in the middle of the study. Detailed investigation revealed that the binding of outer-primers to Flu A targeted sites was disturbed by several recent mutations emerged within the priming sequences. The detection performance was restored after relocating the outer-primers. Hence, it is important to review the genomes of relevant pathogens from time to time, and update assay design if required. The proposed biochemistry protocol, materials and PCR conditions have been verified and adopted in clinical diagnostic use and therefore is justified to be clinically relevant.

IEEE Journal of Translational Engineering in Health and Medicine

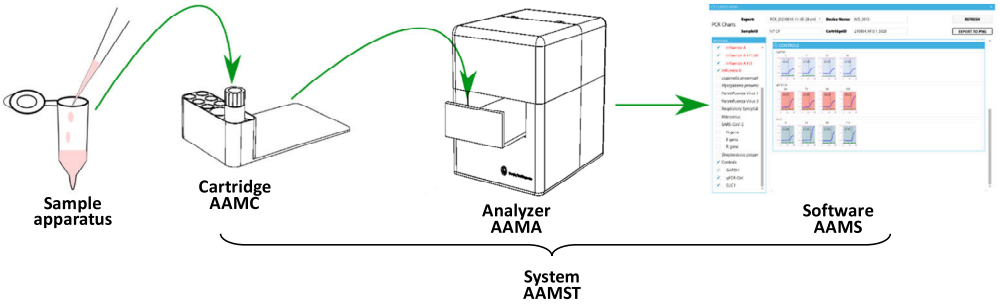

FIGURE 2. Components and workflow of the Avalon Automated Multiplex System (AAMST). Sample is added into a sample apparatus and inserted into the AAMC cartridge. After loading the cartridge into the AAMA analyzer, the whole testing procedure is automated and controlled by an operator through the AAMS software. At the end of biochemistry procedures, the software performs data analysis and result are visualized.

TABLE 2. Pathogens and corresponding gene targets of 23-plex nested RT-qPCR used in clinical evaluation study.

Pathogens	Abbreviation	Gene target (s)	Replicates[1]
Adenovirus	AdV	Hexon	6
Influenza A (Matrix)[2]	Flu A	Matrix	6
Influenza A (pdm09 H1)	Flu A/H1-2009	Hemagglutinin	6
Influenza A (H3)	Flu A/H3	Hemagglutinin	6
Influenza B	Flu B	Matrix	6
Middle East Respiratory Syndrome coronavirus	MERS-CoV	Nucleoprotein (NP)	4
Metapneumovirus	hMPV	Nucleoprotein (NP)	6
Parainfluenza 1	hPIV 1	Nucleoprotein (NP)	6
Parainfluenza 3	hPIV 3	Nucleoprotein (NP)	6
Respiratory syncytial virus	RSV	Nucleoprotein (NP)	6
Enterovirus	EV	5' UTR	6
Human rhinovirus	RV	5' UTR	6
Severe acute respiratory syndrome coronavirus 2	SARS-CoV-2	Envelope protein (E)	4
		Nucleocapsid phosphoprotein (N)	4
		RNA dependent RNA polymerase (Rdrp)	4
Mycoplasma pneumoniae	MP	P1	6
Legionella pneumophila	LP	Mip	4
Bordetella pertussis	B pertussis	Porinprotein	4
Chlamydophila pneumoniae	CP	16S	6
Streptococcus pyogenes	S pyogenes	spy	6
Quality controls:			
Glyceraldehyde 3-phosphate dehydrogenase mRNA (GAPDH)			4
Schizosaccharomyces pombe RNA (SUC1)			4
qPCR control			4

[1]Number of qPCR replicates (number of lightbulbs)
[2]Generic influenza A assay, regardless of strains.

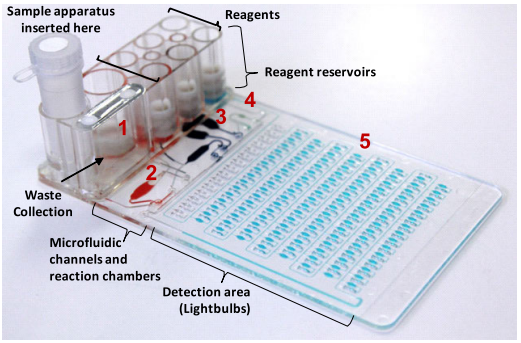

FIGURE 3. Image of AAMC with fluidic paths and reaction chambers visualized by colored dyes. The red numbers (1-5) indicated the corresponding workflow steps in Table 1.

III. THE AVALON AUTOMATED MULTIPLEX SYSTEM

The proposed AAMST comprises Cartridge (AAMC), Analyzer (AAMA) and Software (AAMS). Fig. 2 illustrates its working procedures and are introduced in the following:

A. AVALON AUTOMATED MULTIPLEX CARTRIDGE (AAMC)

The microfluidic cartridge is an enclosed environment where the whole testing process is carried out. A cartridge filled with colour dyes indicating the fluidic channels and reaction chambers is demonstrated in Fig. 3. The cartridge has a footprint area of 85 × 150 mm (width × length) that can be divided into three functional regions: 1) reagent reservoirs, 2) microfluidic channels and reaction chambers, and 3) detection lightbulb area.

In the region of reagent reservoirs, a sample port is defined at the top left corner serving as an interface to the sample apparatus. It is an inlet for sample to enter the cartridge. Vertical cylinders serve as container tubes for reagent storage. Each cylinder has both ends opened. The lower end is closed by a piece of foil. Following reagents filling to the cylinders, syringe plungers are added to the top. After the cartridge is inserted into the analyzer, the syringe plungers are coupled with actuators driven by stepper motors. Vertical movements of syringe plungers act as fluidic pump for controlling flows of reagents with precise volume inside the cartridge. An empty reservoir is included for collecting reaction wastes. Its upper end is closed with a hydrophobic filter for ventilation while retaining liquid waste in the cartridge.

In the region of microfluidic channels and reaction chambers, sample and reagents are directed to respective functional reaction zones through a fluidic network. Its flow paths are controlled by built-in valves. Silica beads and membrane are pre-packaged in the lysis and isolation chambers, respectively, during cartridge production.

In the detection area, 120 individual reaction chambers, namely lightbulbs, are arranged in an 8 × 15 array (row × column). This lightbulb array mimics a 96-well

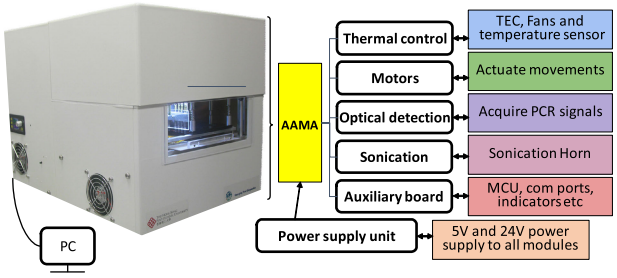

FIGURE 4. AAMA analyzer and its system diagram with the modules connected.

qPCR plate used on benchtop, enabling parallel qPCRs of all pathogen targets and controls in replicates. Each lightbulb is approximately 2.5 μl in volume where singleplex qPCR is performed. A pair of inner-primer and a probe specific to one pathogen are spotted into each lightbulb using a robotic dispensing machine. Real-time qPCRs are set up by mixing the diluted amplicons from first-stage PCR with qPCR master mix from the cartridge reservoir, followed by distributing the mixture among all of the 120 lightbulbs. To achieve uniform distribution in microfluidic mean, a zigzag main channel is routed across the detection area. The 120 lightbulbs are individually branched out from the main channel in parallel through 'T' shape junctions. When a continuous liquid flow in the main channel is blocked at the outlet, the flow starts to enter the lightbulbs. Each of the lightbulb has an air chamber attached. The air chamber can reduce and balance back pressure built up during inflow to an enclosed chamber without a vent. After filling, the inlets of lightbulbs are sealed off by heat. Thermal cycling of second-stage PCR begins and fluorescence signals over the lightbulbs are detected at PCR cycles. The cartridge is disposed after a run is completed. No infectious substance is left in the analyzer.

The cartridges are manufactured by injection molding for ease of mass-production. The plastic materials have critical physical properties, such as being mechanically endurable up to 110°C, allowing high optical transmission for the fluorophore spectra, and chemically inert to the reagents involved. The cartridge is assembled by heat and adhesive-tape bonding. All parts are cleaned and disinfected before assembling. Buffers and reaction master mixes are pre-packed in the reagent reservoirs. Primers and/or probes for RT-PCR and qPCR are pre-spotted and freeze-dried into corresponding reaction chambers.

B. AVALON AUTOMATED MULTIPLEX ANALYZER (AAMA)

The analyzer is a hub of actuators for executing passive components in the cartridge, thermal cycler and signal acquisition unit. In a cubic housing with dimension of 35 × 45 × 40 cm (width × depth × height, Fig. 4), six main modules are integrated. They are:

1) THERMAL CONTROL MODULE

The thermal control module regulates thermal profiles of all biochemical reactions. The module comprises thermoelectric cooler (TEC) elements, a proportional–integral–derivative (PID) controller driver board, and temperature sensors for measuring feedback. This combination forms a closed-loop system to achieve precise temperature output for PCR. High-current (>10 A) module is employed to facilitate rapid ramping of temperature. Ventilation system is designed for effective cooling of heat sinks and maintaining functional temperatures in the analyzer. This thermal module can output temperatures between 20 – 110 °C with maximum ramp-rate of 5°C/sec. To ensure a tight contact between heat block and cartridge for effective heat transfer, a spring-loaded press driven by a high-torque stepper motor is used for pressurizing the cartridge toward the heat block.

2) MOTOR MODULE

The motor module manipulates all mechanical motions inside the analyzer, such as tray-in and -out for cartridge loading, plunger movements, switching fluidic valves, etc. These motions are driven through stepper motors and servo motors. The motors are connected to motor controller boards, which communicate with the control software through a RS-232 serial port. The software assigns commands such as speed and travel distance to respective motors according to the testing protocol.

3) OPTICAL DETECTION MODULE

The optical detection module comprises a cascade of four fluorescence detectors mounted on a x-y movable fixture. Each detector, integrated with miniaturized optical lens system, two fluorophore-specific sets of high-power LED and narrow-band filters, is compact in size and sensitive to measure up to two fluorescent dyes. During the elongation phase of qPCR, each detector walks through one lightbulb after another and captures fluorescent signals. When four detectors are fully installed, signals from four lightbulbs can be measured simultaneously at a time.

4) SONICATION MODULE

The sonication module is set to facilitate sample lysis. It generates ultrasonic vibration that triggers bead bombardment to disrupt cell walls and membranes. A cylindrical ultrasonic horn (7 mm diameter) with 40-kHz output vibration frequency has a fitted contact to the position of lysis chamber of the cartridge. The parameters of sonication time, vibration displacement and contact force are optimized to prevent cartridge deformation due to heat generation.

5) AUXILIARY BOARD

The auxiliary board is designed for coordinating driver boards and extensional functions such as temperature monitoring at different locations inside the analyzer. It is a printed circuit board (PCB) which incorporates a microcontroller (MCU), electronic switches, RS-232 ports, power distribution circuits, wire routing, fuses and pin-sockets for electrical components. In addition, an USB hub is used to centralize all connections from various driver boards in the analyzer. The analyzer and the external stand-alone computer are connected simply with a USB cable.

IEEE Journal of Translational Engineering in Health and Medicine

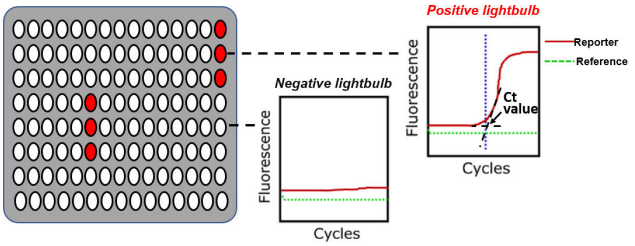

FIGURE 5. Illustration of 8 × 15 lightbulb array for second-stage qPCR. Each lightbulb detects single pathogen targets depending on the pre-spotted primers and probe. For a positive detectable test (red lightbulb), amplification curves are obtained from the reporter dye (red solid lines) showing exponential growth of fluorescence signal. Ct values are further calculated. Baseline signals from reference dye (green dashed lines) are also visualized.

6) POWER SUPPLY UNIT

All electrical components are powered by the power supply unit. It is responsible for converting 220V/110V alternating current (AC) to direct current (DC) of 5 V and 24 V voltages. Its maximum power rating is approximately 700 W.

C. AVALON AUTOMATED MULTIPLEX SOFTWARE (AAMS)

The software is developed as a major interface for operators to access AAMST. It is installed in a stand-alone computer, connecting to the analyzer with a USB cable. Front-end interface is user-friendly for operators to (i) register samples and cartridge information through a keyboard and/or a barcode reader, (ii) start a testing procedure, (iii) monitor all reaction parameters and test progress, (iv) analyze raw data and visualize test result, and (v) compatible to workflow of routine laboratories. Its back end communicates with the analyzer for sending commands and getting returned information. System settings and biochemical reaction protocols can be configured and defined in the software by XML files.

After a test is completed, the software automatically analyzes raw signal intensities acquired by the fluorescence detectors. Fig. 5 illustrates the lightbulb array and qPCR result analyzed by the software. When a pathogen target is present in the sample (red lightbulbs), positive amplification curves with exponential increase in fluorescence signals emitted from the reporter dyes are observed in the lightbulbs of corresponding targets. Such typical amplification curves exhibit three phases, i.e., exponential, linear and plateau phase. In contrast, when a pathogen target is absent (blank lightbulbs), the curves remain flat as no amplification occurs.

Threshold cycle (Ct) values are further calculated for positive lightbulbs. It is defined as the intersection between the extrapolation of maximum slope at linear phase of an amplification curve and its baseline (Fig. 5). The calculation also takes into account of boundary conditions, such as the range of slope values and the magnitude of intensity above baseline, in order to validate the calculated Ct values. By mapping the locations of lightbulbs where amplification curves with valid Ct values appear, pathogens in the sample can be identified. At the end of a test, the analyzed result and a test report are generated by the software.

D. OPERATION AND FLUIDIC SEQUENCE IN THE CARTRIDGE

The fluidic flow inside the cartridge is cooperative interactions between the cartridge with reference to the biochemistry workflow (Table 1):

1) SAMPLE LOADING AND PROCESSING

Three hundred microliters, or maximally 1 mL, of sample is manually loaded into a sample apparatus. In clinical setting, the loading of potentially infectious samples can be carried out inside a biosafety cabinet in order to minimize infectious risk. The sample apparatus is enclosed and inserted into the sample port on a cartridge. It is then placed onto the loading tray of the analyzer. After a run is started by an operator through the software, the entire testing procedure is automated in the analyzer. The loaded sample is first flowed into the lysing chamber, where it is mixed with lysis buffer. The lysis chamber is pre-packaged with silica beads for mechanical cell disruption by sonication. After sample is lysed, it is mixed with nucleic acid binding buffer and passed into the extraction chamber.

2) NUCLEIC ACID EXTRACTION

Nucleic acids, including DNA and RNA, are isolated by passing the lysate through a silica membrane in the extraction chamber. The silica membrane is then washed twice with washing buffers. The bounded nucleic acids are eluted at 65°C by a continuous flow of elution buffer. The segment of eluate that contains the highest amount of nucleic acids and least contaminant is collected for subsequent biochemical reactions. Liquid waste generated after extraction is potentially infectious. It is collected in the waste tank of the cartridge.

3) FIRST-STAGE RT-PCR

Extracted nucleic acids are flowed into the RT-PCR chamber which is already pre-spotted with outer-primers. After mixing with reaction master mix from the reservoir, first-stage multiplex RT-PCR is carried out with thermal cycling controlled by the analyzer.

4) DILUTION AND SECOND-STAGE qPCR

After RT-PCR is completed, a fractional volume of the amplification product is 67-fold diluted with nuclease-free water. It is then mixed with qPCR master mix from the reservoir, and flowed into the 120 lightbulbs where qPCR is carried out.

5) END OF A RUN

After a run is completed, the software automatically analyzes fluorescent data of all lightbulbs, and generates amplification curves and Ct values. A qualitative (presence/absence) pathogen detection report is further generated. Operators can perform additional analysis and retrieve raw data by using the software.

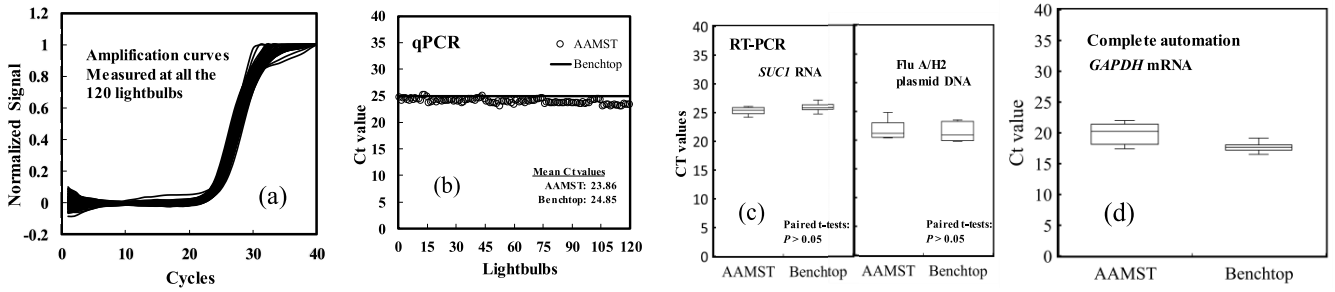

FIGURE 6. Validation of different biochemistry modules in AAMST. (a) The SUC1 template was consistently detected among all of the 120 lightbulbs by the qPCR module. (b) A plot of Ct values of the 120 lightbulbs; (c) Efficiency of RT-PCR was tested with SUC1 RNA and Flu A/H2 plasmid DNA templates; (d) A complete automation from sample processing to qPCR detection using human Hela cells as sample input. GAPDH mRNA was detectable by the system. Ct values obtained from the AAMST agreed well with the benchtop counterpart.

IV. VALIDATION AND RESULT

A. VALIDATION OF INDIVIDUAL BIOCHEMISTRY MODULES

1) CONSISTENCE OF qPCR PERFORMANCE AMONG 120 LIGHTBULBS

Performance of qPCR depends on the capability of the system in (i) consistent volume distribution and effective sealing of each lightbulb, (ii) functioning of detection module, (iii) uniform heat distribution over the heating block and among the lightbulbs, and (iv) stable thermocycling with minimum temperature variation. Thermal performance is particularly critical [26], [27]. Testing template was prepared on benchtop by RT-PCR amplification using outer-primer specific to *SUC1* gene from RNA extracted from *Schizosaccharomyces pombe (S. pombe).* The amplified template was mixed with qPCR master mix and *SUC1* inner-primers and probe. The reaction mixture was loaded into the pre-qPCR chamber of a blank cartridge in which no primers or probes were pre-spotted. The cartridge was then loaded into the analyzer and second-stage qPCR was performed. The steps of system operation included reaction mixture distribution, lightbulb sealing, thermocycling and signal detection. Thermal profile involved an initial denaturation (95°C, 30s), followed by 40 PCR cycles (95°C, 1s and 55°C, 45s). As comparison, an aliquot of the reaction mixture was also run on a benchtop qPCR instrument (QuantStudio 7 Flex Real-Time PCR System, Thermo Fisher).

As shown in Fig. 6a and supplementary Fig. S1 for lightbulb mapping, *SUC1* template was consistently amplified among all of the 120 lightbulbs. A relatively small variation of Ct values was obtained with a standard deviation (SD) of 0.45 (Fig. 6b). In addition, the average Ct value of the lightbulbs (23.86) was comparable to that of the benchtop (24.85). The result hence demonstrated the accuracy and consistency of the qPCR module of the system.

2) PERFORMANCE OF RT-PCR

In this evaluation, testing template was prepared by combining 8 pg of *S. pombe* RNA and 0.01 pg of Influenza A/H2 (Flu A/H2) plasmid DNA. It is worth noting that both RT and PCR were essential for *S. pombe* RNA detection; whereas only PCR was necessary for Flu A/H2 plasmid DNA detection. RT-PCR reaction mixture was setup by mixing the template, RT-PCR master mix and outer-primers targeting *SUC1* and hemagglutinin genes for *S. pombe* and Flu A/H2, respectively. The reaction mixture was added into the RT-PCR chamber of the cartridge where no primers were pre-spotted. RT-PCR was then carried out by the analyzer. Thermal profile involved RT (48°C, 600 s), RT inactivation (95°C, 600 s) and 20 PCR cycles (95°C, 15 s and 65°C, 45 s). After the reaction, RT-PCR product was collected from the cartridge. The product was diluted 67-fold with nuclease-free water before running qPCR on the benchtop instrument (QuantStudio 7 Flex Real-Time PCR System, Thermo Fisher). An aliquot of RT-PCR reaction mixture was also run in parallel on a benchtop thermocycler (Veriti Thermal Cycler and QuantStudio 7 Real-Time PCR System, Thermo Fisher) for comparison. Result from ten replicated sets of experiments was showed in Fig. 6c. For both templates used, the quantities of RT-PCR products amplified by the system and on benchtop were similar with no statistically significant differences ($P = 0.065$ for *SUC1*, $P = 0.272$ for Flu A/H2, paired t-tests). For *SUC1* RNA, the Ct values (mean $\pm$ SD) were 25.37 $\pm$ 0.58 (AAMST) versus 25.84 $\pm$ 0.62 (benchtop); whereas for Flu A/H2 plasmid DNA, the Ct values were 21.59 $\pm$ 1.11 (AAMST) versus 21.40 $\pm$ 1.42 (benchtop). The result indicated that RT-PCR efficiency of the system was similar to that performed on benchtop.

3) VALIDATION OF A COMPLETE AUTOMATION

Complete automation is analytically evaluated by examining the efficiency of measuring *glyceraldehyde 3-phosphate dehydrogenase* (*GAPDH*) mRNA, a widely used housekeeping human gene expressed across different organs and in different pathological and physiological conditions, from human Hela cells. The cartridges used in this experiment were pre-spotted with its specific primers and probes for RT-PCR and qPCR. All reagents were packaged in the cartridge reservoirs. To prepare the testing sample, in-house cultured Hela cells were mixed in viral transport medium (VTM) at a concentration of 500 cells per 300 μL, a concentration that is usually observed in human clinical samples. The test followed the procedures in Section III-D. As comparison, RNA was separately extracted from the Hela-cell sample on benchtop by using QIAamp MinElute Kit (Qiagen) following manufacturer's instructions. The benchtop-extracted RNA

IEEE Journal of Translational Engineering in Health and Medicine

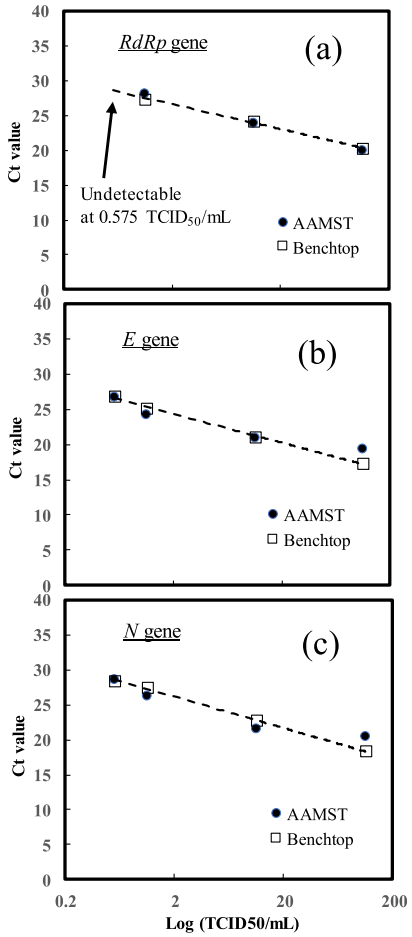

FIGURE 7. Plots of Ct values against log concentrations of SARS-CoV-2 viral loads. (a) RdRp gene, (b) E gene and (c) N gene were measured by AAMST and on benchtop. Four serial dilutions with concentrations of 0.575, 1.15, 11.5 and 115 TCID50/mL were tested. The dash lines show linear regressions along the benchtop data.

was then loaded into the cartridge, followed by RT-PCR and qPCR performed by the analyzer. A total of eight replicates of the AAMST-benchtop pairwise experiments were carried out.

The result was shown in Fig. 6d. *GAPDH* mRNA was robustly detected in all of the eight replicated Hela-cell samples processed by the system. The dataset was further examined quantitatively and observed that the Ct values obtained from the system were larger than those from the benchtop ($P < 0.05$, paired t-test), with an average Ct value difference of 2.32 (20.00 ± 1.6 for AAMST, 17.68 ± 0.73 for benchtop). The finding implied that *GAPDH* mRNA amount extracted by the system may be reduced when compared to those on benchtop. Further examination and adjustment of extraction parameters will be performed in order to improve the yield. The result validated the fluidic operation, a collective performance resulted from all of the hardware and software.

B. PERFORMANCE OF MULTIPLEXED PATHOGEN DETECTION

To demonstrate multiplexing feasibility, a 23-plex testing assay was designed for detecting 20 pathogen targets and 3 quality controls (Table 2). The pathogen targets covered

TABLE 3. Result of Multiplexed pathogen detection.

	Sample with pathogen targets	Negative control sample
FLU A	28.3,27.4,28.2,27.9,28.6,27.7 (28.0)	Undetermined
FLU A/H1	22.3,21.8,22.4,21.7,22.5,21.6 (22.1)	Undetermined
FLU A/H3	22.1,21.8,21.8,21.5,21.6,21.4 (21.7)	Undetermined
FLU B	21.9,21.3,21.1,21.1,20.9,21.3 (21.3)	Undetermined
CP	22.6,22.8,23.0,22.4,22.9,22.7 (22.7)	Undetermined
SUC1	26.0,25.5,26.2,27.3 (26.3)	24.4,24.7,25.5,25.4 (25.0)
GAPDH	21.0,19.6,20.8,20.1 (20.4)	20.6,20.4,20.4,20.1 (20.4)
QPCR	26.0,25.6,25.0,25.1 (25.4)	24.8,23.6,23.1,24.4 (24.0)

Average of the Ct values is embraced with parentheses ( ).

viruses (e.g. SARS-CoV-2 and influenza) and bacteria (e.g. *Streptococcus pyogenes*). Inside the cartridge, 23 pairs of outer-primers were pre-spotted in the RT-PCR chamber for performing a 23-plex RT-PCR. Each lightbulb in the qPCR module was pre-spotted with a pair of inner-primers and a probe for measuring one pathogen target. Among the 120 lightbulbs, four to six lightbulbs were used for each pathogen detection, while four lightbulbs were used for each quality control (Table 2). As a RT-PCR control, *SUC1* RNA was added into RT-PCR master mix in the reservoir during cartridge production. qPCR control is an oligonucleotide with arbitrary sequence. It was spotted with corresponding primers and probe in designated lightbulbs.

An artificial sample containing nucleic acids from five pathogen targets were prepared by mixing in-vitro transcribed RNAs of Flu A, Flu A/H1, Flu A/H3, Flu B, plasmid DNA of CP, and total RNA from Hela cells. The full testing procedures were carried out by the system. A negative control that contained Hela-cell RNA only was also tested.

The testing result was listed in Table 3 and shown in supplementary Fig. S2a for lightbulb mapping. All of the five pathogen nucleic acids were robustly detected with valid amplification curves and Ct values in all of the replicated qPCR lightbulbs. Positive signals were also obtained for all of the three quality controls, confirming validity of the run. The Ct values measured by the system agreed well with their benchtop counterparts. On the other hand, no amplification was observed for non-target lightbulbs, implying no cross-reactivity among the pathogen assays being multiplexed. This would be attributed to appropriate primer-probe design and stringent thermal profiling during PCRs. No crosstalk was observed across the lightbulbs, indicating reliable sealing performance. Automatic multiplexing detection of the system was hence demonstrated.

For the negative control sample (Table 3 and S2b), no amplification and valid Ct value of pathogen targets were observed, confirming specificity of the test. The Ct values of the controls fell within an acceptable range based on data of previous runs, confirming consistency of the full runs. Each quality control indeed monitors the validity of its corresponding testing sub-process. *GAPDH* mRNA reflects sample quality and extraction efficiency. *SUC1* RNA is an in-process control for first-stage RT-PCR, including its reaction master mix, thermal cycling condition and fluidics flow. qPCR control verifies the running of second-stage qPCR includes proper reaction master mix, lightbulb reaction setup

TABLE 4. Information of clinical specimens included in clinical evaluation.

	Negative samples	Positive samples
Total no. of clinical samples	50	13
Nasopharyngeal aspirate (NPA)	26	2
Nasopharyngeal swab (NPS)	23	8
Deep throat saliva (DTS)	0	3
Endotracheal aspirate (ETA)	1	0

and thermal cycling. The result of the quality controls is used for passing or failing a test run in order to avoid incorrect result due to system malfunction. In particular, negative result of a sample can be confidently called if all of the three controls are passed. The controls are also useful to narrow down the cause of failure in a sub-process level.

C. ADVANTAGE OF A MULTIPLEX ASSAY FOR SARS-CoV-2

Advantages of COVID-19 diagnosis with a multiplex assay was demonstrated. The assay targets three gene regions of SARS-CoV-2, namely, *RNA-dependent RNA polymerase (RdRp), envelope protein* (*E*) *and nucleocapsid protein* (*N*) genes. These are SARS-CoV-2 conserved regions that are widely used in benchtop-based RT-PCR diagnostic tests. Heat-inactivated SARS-CoV-2 culture fluid (ZeptoMetrix Corporate, Buffalo, US) was serially diluted to concentrations of 0.575, 1.15, 11.5 and 115 $TCID_{50}$/mL and analyzed by the system. For all of the three SARS-CoV-2 gene targets, the system showed sensitivities similar to the benchtop counterparts (Fig. 7). The lowest detectable concentrations were 0.575 $TCID_{50}$/mL for *E* and *N* genes, and 1.15 $TCID_{50}$/mL for *RdRp* gene. The result indeed agreed with Vogels et al. [28] that detection assay targeting *RdRp* showed lower sensitivity than other tested gene regions. The result also demonstrated the benefit of multi-target detection in enhancing reliability of pathogen detection. Simultaneous detection of multiple sites of a pathogen can reduce false negative result due to recurrent genetic mutations [28]. In addition, the result in Fig. 7 reveals that the Ct values are linearly proportional to the concentrations as measured by the system. The finding hence suggested the potential of the system for quantitative pathogen analysis, such as viral load measurement.

It is worth noting that, in Section IV-A to IV-C, all the testing samples involved were non-clinical and safe to use in laboratory. For safety reason, it is essential to assure integrity of the system before running clinical samples.

D. EVALUATION WITH CLINICAL SAMPLES

Human samples obtained clinically were relatively complex due to the presence of PCR inhibitors, intactness and varied abundance of nucleic acids, and the potential existence of diverse pathogen strains that share similar genomic sequences [29]. In the system evaluation, the sample cohort included various types of specimens (Table 4), 50 negative specimens and 13 specimens positive for pathogen infection as diagnosed by standard methods in Department of Microbiology, Queen Mary Hospital. The use of the clinical samples was approved by the local Institutional Review Board.

TABLE 5. Clinical evaluation Result of positive clinical samples.

Sample	Type	Diagnosed pathogen	AAMST testing			
			Positive pathogen targets (Ct values)			*GAPDH* mRNA (Ct values)
			E	*N*	*Rdrp*	
1	NPS	SARS-CoV-2	23.1	24.3	23.3	21.1
2	NPS	SARS-CoV-2	22.4	24.3	23.0	22.0
3	NPS	SARS-CoV-2	27.6	34.4	24.5	25.4
4	NPS	SARS-CoV-2	24.5	27.0	27.0	25.4
5	NPS	SARS-CoV-2	25.1	26.7	26.8	23.2
6	NPS	SARS-CoV-2	21.6	23.4	23.8	16.6
7	NPS	SARS-CoV-2	25.4	29.2	32.3	29.2
8	DTS	SARS-CoV-2	22.8	25.1	26.0	22.9
9	DTS	SARS-CoV-2	22.5	25.7	24.5	21.4
10	DTS	SARS-CoV-2	26.0	31.0	29.8	24.6
11	NPA	Flu A/H1	Flu A (26.0), Flu A/H1 (15.8)			26.0
12	NPS	Flu B	Flu B (24.3)			24.7
13	NPA	RSV	RSV (15.0)			18.9

Each specimen was first immersed in a container with VTM. It was then loaded into the sample apparatus and sent to the system for analysis following the operation in Section III-D. In the negative samples, *GAPDH* mRNA was detected in all of the 50 samples by the system. The mean AAMST Ct values (22.38) were larger than that in benchtop control (19.17) by a difference of 3.21 (Fig. 8a), possibly due to the reduced nucleic acid extraction yield of AAMST (Fig. 6d). This suggested that the system exhibited unique PCR linearity and the lowest detection limit (LOD) differing from the benchtop assay. Therefore, at a later stage, the clinical sensitivity and specificity of the system have to be defined statistically by considering a significant number of clinical samples with a wide range of concentrations and sample types. In this small group feasibility study, accuracy of the detection equivalent to the benchtop was achieved. The pairwise Ct values were closely correlated with each other (Pearson correlation test, $P < 0.05$ and correlation coefficient, $r = 0.65$) (Fig. 8b). No amplification signal was observed for all of the pathogen targets, verifying the system specificity.

From the positive samples collected from patients, 10 infected with COVID-19, the system consistently detected RNAs derived from the *E*, *N* and *Rdrp* genes of SARS-CoV-2 (Table 5). The other 3 infected with common upper respiratory pathogens (Flu A/H1, Flu B and RSV) are also identified. The AAMST result agreed well with that diagnosed clinically using conventional laboratory methods. This result validated the capability of the system in testing clinical samples, achieving multiple detections for the targets of SARS-CoV-2, subtype influenza strains, and other respiratory pathogens that manifest similar clinical symptoms.

In conventional laboratory, operation time is at least around 5 – 6 hours which includes reagent preparation, centrifuges, transferring from one equipment to another, PCR run time etc. time could be longer when logistic of samples is needed. Since the cartridge has all the reagents pre-packed and the analyzer can be located at the point of a test, for

IEEE Journal of Translational Engineering in Health and Medicine

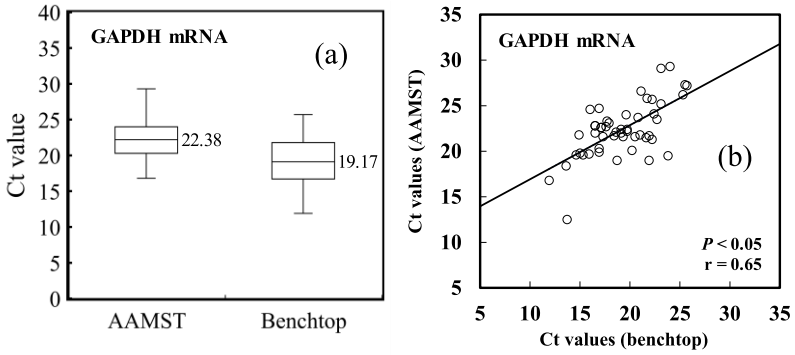

FIGURE 8. GAPDH mRNA concentrations of 50 negative clinical samples as measured by AAMST. (a) GAPDH mRNA concentrations measured by AAMST were lower than that by the benchtop method. (b) Ct values between AAMST and the benchtop method were closely correlated with Pearson correlation test (P) < 0.05 and correlation coefficient (r) = 0.65.

the most optimized case, the run time can be as short as ∼1 hour and can be further shortened by optimization in the biochemistry and the system parameters. The system has showed advantage in the testing duration.

V. DISCUSSION

A rapid and accurate on-site POCT would facilitate doctors to implement early clinical management [8], [23]. Healthcare providers can also offer the test to the public without expensive investment in setting up molecular laboratories. A testing site requires, in a market range, only tens of thousands USD to equip the analyzer and a hundred USD for a cartridge, significantly reducing the entry barrier of molecular diagnostic. Cost per test is the key factor for popularization of this technology. Cost down to tens USD per test is the range to be reached at a later stage of mass production.

COVID-19 pandemic has illustrated the importance and demand of the system proposed in this work. It fulfills the current medical needs of infection screening, diagnosis and surveillance. The multiplex testing assay can also be readily updated when new pathogens or strains emerge.

One major challenge of this development is to deliver a highly multiplexed assay that retains sensitivity and specificity of detection. Thorough optimization of different biochemical components had been carried out, such as primer and probe sequences, reagent recipes, reaction conditions, and production of reference controls. Optimization effort increased exponentially with the number of targets to be multiplexed. A comprehensive evaluation of biochemistry performance of the system will be presented in subsequent report.

Due to the hurdles in biochemistry and engineering, many POCT systems available in the market detect only one or a few pathogens in a single reaction [23], [30]. In contrast, AAMST would offer a choice for simultaneous profiling of a large panel of pathogens in a sample. Such ‘‘pathogen profiling’’ approach is valuable in many scenarios [3], [31]. For instance, during the current COVID-19 pandemics, symptomatic individuals and at-risk people such as close-contact of confirmed cases are usually tested for SARS-CoV-2 only by conventional POCT. With the use of AAMST, the screening of causative pathogens can be extended to many other important respiratory tract pathogens. This would allow a more comprehensive infection diagnosis and reduce anxiety of subjects of concern.

Another example is the guidance of clinical treatment. AAMST is capable of distinguishing bacterial from non-bacterial infection for empirical antibiotic prescription. The more efficient use of antibiotics could reduce the chance of bacterial resistance from developing [8].

Apart from infection diagnosis, AAMST can be readily adapted with biochemical assays for other applications, such as drug-resistant genes in bacteria and tumoral mutations in cancers. In the aspect of engineering, the capacity of multiplexing can further be enhanced by increasing the number of lightbulbs following same design rule and microfluidic operation. Further development of optical system is also critical. The overall system performance and turnaround time could be significantly enhanced by adding more detection channels with faster signal acquisition. The current AAMST is a compromised design among space, number of optical channels, sensitivity and speed.

In term of throughput, the current system is certainly high in the number of detecting pathogens in a test but is rather low for capacity in handling many samples at a time. For the site demanding high capacity, many analyzers are needed. This will take up space. Therefore, evolution will necessarily include engineering design of operating multiple cartridges in a single equipment. Assay and system specifications generated in this work will be useful for such high throughput version in the future.

The feasibility and clinical utility of AAMST was demonstrated in this report. Large-scale analytical and clinical validation and evaluation of the system will be followed in order to define the system specifications for regulatory approval.

VI. CONCLUSION

In conclusion, the AAMST system (comprising AAMC cartridge, AAMA analyzer and AAMS software) was developed for automating a nested RT-qPCR protocols for detecting a

large number of targeted nucleic acid sequences. The system has been validated analytically using cultured cells and fluid, in-vitro transcribed RNA and plasmid DNA with excellent agreement to the benchtop counterparts. Detection results from clinical samples including those infected by SARS-CoV-2 and several other important respiratory pathogens have also fully agreed with gold standard testing methods. The current feasibility study demonstrated the clinical usefulness of AAMST and it can potentially be deployed in many applications that require multiplexed nucleic acid detection in both research and clinical settings.

ACKNOWLEDGMENT

The authors would like to thank all the members of the Emerging Viral Diagnostics (HK) Ltd. and Drs. Nancy BY Tsui and Anita Yee for their help in the preparation of this manuscript, and also would like to thank the members in The Hong Kong Polytechnic University and the Department of Microbiology, The University of Hong Kong for their support to the experiments, and also would like to thank the generous support from Antony Leung Kam Chung and the Emerging Viral Research Foundation.

REFERENCES

[1] D. E. Bloom and D. Cadarette, "Infectious disease threats in the twenty-first century: Strengthening the global response," *Frontiers Immunol.*, vol. 10, p. 549, Mar. 2019.

[2] Y. C. Wu, C. S. Chen, and Y. J. Chan, "The outbreak of COVID-19: An overview," *J. Chin. Med. Assoc.*, vol. 83, no. 3, pp. 217–220, Mar. 2020.

[3] B. D. Kevadiya et al., "Diagnostics for SARS-CoV-2 infections," *Nature Materials*, vol. 20, no. 5, pp. 593–605, May 2021.

[4] O. Vandenberg, D. Martiny, O. Rochas, A. van Belkum, and Z. Kozlakidis, "Considerations for diagnostic COVID-19 tests," *Nature Rev. Microbiol.*, vol. 19, no. 3, pp. 171–183, Mar. 2021.

[5] C. M. Ackerman et al., "Massively multiplexed nucleic acid detection with Cas13," *Nature*, vol. 582, no. 7811, pp. 277–282, Jun. 2020.

[6] S. Sridhar et al., "A systematic approach to novel virus discovery in emerging infectious disease outbreaks," *J. Mol. Diagnostics*, vol. 17, no. 3, pp. 41–230, May 2015.

[7] A. Hematian et al., "Traditional and modern cell culture in virus diagnosis," *Osong Public Health Res. Perspect.*, vol. 7, no. 2, pp. 77–82, Apr. 2016.

[8] K. J. Land, D. I. Boeras, X.-S. Chen, A. R. Ramsay, and R. W. Peeling, "REASSURED diagnostics to inform disease control strategies, strengthen health systems and improve patient outcomes," *Nature Microbiol.*, vol. 4, no. 1, pp. 46–54, Dec. 2018.

[9] V. R. Carr and C. Chaguza, "Metagenomics for surveillance of respiratory pathogens," *Nature Rev. Microbiol.*, vol. 19, no. 5, p. 285, May 2021.

[10] A. Cassedy, A. Parle-McDermott, and R. O'Kennedy, "Virus detection: A review of the current and emerging molecular and immunological methods," *Frontiers Mol. Biosciences*, vol. 8, Apr. 2021, Art. no. 637559.

[11] L. Zou et al., "SARS-CoV-2 viral load in upper respiratory specimens of infected patients," *New England J. Med.*, vol. 382, no. 12, pp. 1177–1179, Mar. 2020.

[12] G. Guglielmi, "Fast coronavirus tests: What they can and can't do," *Nature*, vol. 585, no. 7826, pp. 496–498, Sep. 2020.

[13] S. Pickering et al., "Comparative performance of SARS-CoV-2 lateral flow antigen tests and association with detection of infectious virus in clinical specimens: A single-centre laboratory evaluation study," *Lancet Microbe*, vol. 2, no. 9, pp. e461–e471, Sep. 2021.

[14] W. Leber, O. Lammel, A. Siebenhofer, M. Redlberger-Fritz, J. Panovska-Griffiths, and T. Czypionka, "Comparing the diagnostic accuracy of point-of-care lateral flow antigen testing for SARS-CoV-2 with RT-PCR in primary care (REAP-2)," *eClinicalMedicine*, vol. 38, Aug. 2021, Art. no. 101011.

[15] S. Raja et al., "Technology for automated, rapid, and quantitative PCR or reverse transcription-PCR clinical testing," *Clin. Chem.*, vol. 51, no. 5, pp. 882–890, May 2005.

[16] M. A. Poritz et al., "FilmArray, an automated nested multiplex PCR system for multi-pathogen detection: Development and application to respiratory tract infection," *PLoS ONE*, vol. 6, no. 10, Oct. 2011, Art. no. e26047.

[17] M. R. Green and J. Sambrook, "Nested polymerase chain reaction (PCR)," *Cold Spring Harbor Protocols*, vol. 2019, no. 2, pp. 175–178, Feb. 2019.

[18] L. Yamamoto et al., "Performance of a multiplex nested polymerase chain reaction in detecting 7 pathogens containing DNA in their genomes associated with congenital infections," *Arch. Pathol. Lab. Med.*, vol. 144, no. 1, pp. 99–106, Jan. 2020.

[19] R. Wölfel et al., "Virological assessment of hospitalized patients with COVID-2019," *Nature*, vol. 581, no. 7809, pp. 465–469, May 2020.

[20] B. Deepachandi, S. Weerasinghe, P. Soysa, N. Karunaweera, and Y. Siriwardana, "A highly sensitive modified nested PCR to enhance case detection in leishmaniasis," *BMC Infectious Diseases*, vol. 19, no. 1, p. 623, Jul. 2019.

[21] J. Parker et al., "Analytical sensitivity comparison between singleplex real-time PCR and a multiplex PCR platform for detecting respiratory viruses," *PLoS ONE*, vol. 10, no. 11, Nov. 2015, Art. no. e0143164.

[22] I. M. Mackay, "Real-time PCR in the microbiology laboratory," *Clin. Microbiol. Infection*, vol. 10, no. 3, pp. 190–212, Mar. 2004.

[23] C. D. Chin et al., "Microfluidics-based diagnostics of infectious diseases in the developing world," *Nature Med.*, vol. 17, no. 8, pp. 1015–1019, Jul. 2011.

[24] H. Kim, H. J. Huh, E. Park, D.-R. Chung, and M. Kang, "Multiplex molecular point-of-care test for syndromic infectious diseases," *BioChip J.*, vol. 15, no. 1, pp. 14–22, Mar. 2021.

[25] S. Fujimoto, Y. Nakagami, and F. Kojima, "Optimal bacterial DNA isolation method using bead-beating technique," *Memoirs Kyushu Univ. Dep. Health Scissors Med. Sci.*, vol. 3, pp. 33–38, Jan. 2004.

[26] D. R. Almassian, L. M. Cockrell, and W. M. Nelson, "Portable nucleic acid thermocyclers," *Chem. Soc. Rev.*, vol. 42, no. 22, pp. 98–8769, Nov. 2013.

[27] C.-S. Liao, "Miniature RT-PCR system for diagnosis of RNA-based viruses," *Nucleic Acids Res.*, vol. 33, no. 18, pp. e156–e156, Oct. 2005.

[28] C. B. F. Vogels et al., "Analytical sensitivity and efficiency comparisons of SARS-CoV-2 RT–qPCR primer–probe sets," *Nature Microbiol.*, vol. 5, no. 10, pp. 1299–1305, Oct. 2020.

[29] C. Schrader et al., "PCR inhibitors—Occurrence, properties and removal," *J. Appl. Microbiol.*, vol. 113, no. 5, pp. 26–1014, Nov. 2012.

[30] I. V. Jani et al., "Multiplexed immunoassays by flow cytometry for diagnosis and surveillance of infectious diseases in resource-poor settings," *Lancet Infectious Diseases*, vol. 2, no. 4, pp. 243–250, Apr. 2002.

[31] M. G. Becker, T. Taylor, S. Kiazyk, D. R. Cabiles, A. F. A. Meyers, and P. A. Sandstrom, "Recommendations for sample pooling on the cepheid GeneXpert® system using the cepheid Xpert® xpress SARS-CoV-2 assay," *PLoS ONE*, vol. 15, no. 11, Nov. 2020, Art. no. e0241959.